Proceeding of the 2004 American Control Conference
Boston, Massachusetts June 30 - July 2, 2004

Continuous-time control of distributed processes via microscopic simulations*

Antonios Armaou
Department of Chemical Engineering
Pennsylvania State University, University Park, PA 16802

Abstract— **A continuous-time feedback controller design methodology is developed for distributed processes, whose dynamic behavior can be described by microscopic evolution rules. Employing the micro-Galerkin method to bridge the gap between the microscopic-level evolution rules and the "coarse" process behavior, "coarse" process steady states are estimated and nonlinear process models are identified off-line through the solution of a series of nonlinear programs. Subsequently, optimal feedback controllers are designed, on the basis of the nonlinear process model, that enforce stability in the closed-loop system. The method is used to control a system of coupled nonlinear one-dimensional PDEs (the FitzHugh-Nagumo equations), widely used to describe the formation of patterns in reacting and biological systems. Employing kinetic theory based microscopic realizations of the process, the method is used to design output feedback controllers that stabilize the FHN at an unstable, nonuniform in space, steady state.**

I. Introduction

An important research area that has received a lot of attention in recent years is controller design for distributed processes, mathematically modeled by nonlinear dissipative partial differential equation (PDE) systems. One of the research directions involves the development of methods for controller design based on reduced-order models [3], [7], [2] (e.g., obtained using linear or nonlinear Galerkin's methods [15], [18]) that capture the dominant dynamics of the process and can be solved numerically in real time. An accurate, explicit process model is the main prerequisite for the derivation of the reduced-order models, which are used for controller design and real-time implementation.

However, the behavior of an expanding range of distributed processes (for which explicit coarse level mathematical models are unavailable, albeit in principle possible) is being mathematically described using microscopic level simulations (e.g., Lattice Boltzmann, kinetic Monte Carlo, molecular dynamics). The lack of an explicit process model precludes the successful use of standard controller design methodologies for distributed parameter systems to such processes.

Motivated by this, linear discrete-time controller design methodologies were recently developed for lumped [19] and distributed [4] processes described by microscopic evolution rules, utilizing the so-called "coarse time-stepper" approach, developed by Kevrekidis and coworkers [21], [11], [20], that circumvents the derivation of the closed form macroscopic PDEs for the process and identifies the essential coarse-scale system behavior.

Other model reduction approaches of systems described by microscopic evolution rules include approaches for model reduction of the Master Equation [8], the use of wavelets for kMC model reduction [9] and the development of hybrid models for epitaxial growth [16] and crack propagation in materials [5]. In [13], [14], observers based on Monte-Carlo simulations and process measurements were successfully designed to capture the dynamic behavior of microscopic process variables leading to output feedback controller designs.

This work addresses the issue of continuous-time controller design to regulate the coarse properties of processes whose dynamic behavior can be described by microscopic evolution rules. Under the assumption that an underlying closed-form process model is, in principle, possible, however unavailable, micro-Galerkin method [11] is employed to bridge the gap between the microscopic-level evolution rules and the "coarse" process behavior. The derived black-box time-steppers are linked with equation-free methods (such as Recursive Projection Method (RPM) [17] to obtain estimates of the process stationary states, the slow evolving eigendirections in their neighborhood and a discrete-time reduced-order linear model. Nonlinear continuous-time models are subsequently identified off-line through the *solution of a series of nonlinear programs*. Finally, optimal output-feedback controllers are designed that enforce stability of the target, RPM identified, stationary states in the closed-loop system. The proposed approach is validated on a system of coupled nonlinear one-dimensional PDEs (the FitzHugh-Nagumo equations), widely used to describe the formation of patterns in reacting and biological systems. Employing microscopic, kinetic theory based, realizations of these systems to describe the process behavior, the proposed approach stabilizes the unstable, nonuniform in space, steady (microscopically stationary) state, in the presence of open-loop oscillatory behavior.

II. Preliminaries

We consider nonlinear dissipative partial differential equation (PDE) systems whose long-term dynamics can be accurately captured by a few slow-evolving degrees of

*Financial support for this work from the Pennsylvania State University, Chemical Engineering Department, is gratefully acknowledged.
e-mail: armaou@psu.edu

0-7803-8335-4/04/$17.00 ©2004 AACC

freedom, and are of the following form, when represented in an appropriate Hilbert space

$$\begin{aligned} \dot{x} &= \mathcal{L}(x) + \bar{f}(x) + \mathcal{B}(x)u, \quad x(0) = x_0 \\ y_m &= \mathcal{S}x \end{aligned} \tag{1}$$

where $x \in D(\mathcal{L})$ is the state vector, $u \in \mathbb{R}^m$ is the vector of manipulated inputs, and $y_m \in \mathbb{R}^q$ is the vector of the measured outputs. $\mathcal{L}(\cdot)$ is a dissipative, possibly nonlinear, spatial differential operator which includes higher-order spatial derivatives, $\bar{f}(x)$ is a nonlinear vector function of the state, and $\mathcal{B}(x)$ is the actuator distribution function, $\mathcal{S}$ is the measurement sensor shape function, and l is the length of the domain. $D(\mathcal{L}) \subset L^2[0,l]$ is the set of $\mathcal{C}^{o-1}$ functions in $L^2[0,l]$ that satisfy the boundary conditions of the spatial operator and o is the highest order differential of $\mathcal{L}$. Without loss of generality we assume that the target steady state of the system is the origin.

An implicit assumption in the above system description is that the rest, infinite, degrees of freedom of the PDE are strongly stable and, furthermore, the associated dynamics quickly become negligible and can be captured by algebraic functions of the slow-evolving states of Eq.1.

The Kronecker product between matrices $A \in \mathbb{C}^{N\times M}$ and $B \in \mathbb{C}^{L\times K}$ can be defined as a matrix $C \in \mathbb{C}^{(NL)\times(MK)}$

$$C = A \otimes B \equiv \begin{bmatrix} a_{1,1}B & a_{1,2}B & \cdots & a_{1,M}B \\ a_{2,1}B & a_{2,2}B & \cdots & a_{2,M}B \\ \cdots & \cdots & \cdots & \cdots \\ a_{N,1}B & a_{N,2}B & \cdots & a_{N,M}B \end{bmatrix} \tag{2}$$

We also define the k-th order Kronecker product as $A^{[k]} = A^{[k-1]} \otimes A$, $A^{[1]} = A$ and $A^{[0]} = 1$. Finally, $I_n \in \mathbb{R}^{n\times n}$ is defined as the unitary matrix of dimension n and $(\cdot)^*$ denotes the conjugate transpose.

III. Output feedback controller design

We focus on the design of continuous-time output feedback controllers for distributed processes that can, in principle, be mathematically modeled by dissipative PDEs, but are unavailable in closed-form. The PDEs in question are in essence closed-form macroscopic equations for the moments of microscopically evolving (through, say, molecular dynamics, kinetic Monte-Carlo or kinetic theory based codes) distributions.

The controller design is achieved in two stages. During the first stage, the coarse time-steppers, through a "lift-evolve-restrict" procedure provide us with a bridge between macroscopic scale system properties and microscopic evolution simulations; during this system identification step, the process stationary states are identified (using numerical algebra methods such as recursive projection method [17]) and after variance reduction, a coarse slow discrete-time linearization (i.e. the coarse slow eigenvalues and the corresponding eigenvectors) is derived. The reporting horizon of the microscopic scale simulations is an important parameter in the above approach for the identification of the important, slow evolving, spatial patterns, a result of the slaving of the fast dynamics to the dominant ones. Linear continuous-time observers that identify the essential coarse process behavior are subsequently constructed by manipulating the reporting horizon. Issues arising from the transition of the discrete time identified linear behavior to continuous time observers are addressed. During the second stage, output-feedback continuous-time controllers are designed using established methodologies.

A. Off-line identification

1) Problem formulation: To simplify the required notation, we represent the unknown, finite dimensional, slow evolving dynamical system of Eq.1 in the form

$$\dot{x} = f(x) + \sum_{j=1}^{m} u_j(t) \tag{3}$$

where $x \in \mathcal{H}_s$ is the state, $u_j(t)$, is the j-th element of u, $f(x) = \mathcal{L}(x) + \bar{f}(x)$ is a nonlinear vector function, and $g_j(x)$ is the j-th actuator distribution function. $\mathcal{H}_s$ is an n-th dimensional Hilbert subspace spanned by the eigenfunctions associated to the slow eigenvalues of $\mathcal{L}$.

Applying McLaurin series expansion to $f(x)$, $g_j(x)$ we obtain

$$\begin{aligned} f(x) &= \sum_{k=1}^{\infty} \frac{1}{k!} \partial f_{[k]}|_{x=0} x^{[k]} \\ g_j(x) &= g_j(0) + \sum_{k=1}^{\infty} \frac{1}{k!} \partial g_{j\,[k]}|_{x=0} x^{[k]} \end{aligned} \tag{4}$$

where $\partial f_{[k]}|_{x=0} \in \mathbb{C}^{n\times(n^k)}$ and $\partial g_{j\,[k]}|_{x=0} \in \mathbb{C}^{n\times(n^k)}$ are the k-th partial derivatives of $f(x)$ and $g(x)$ with respect to x, respectively, evaluated at $x = 0$. To simplify the notation we denote $A_k \equiv (1/k!)\partial f_{[k]}|_{x=0}$, $B_{j\,k} \equiv (1/k!)\partial g_{j\,[k]}|_{x=0}$, $\forall k$ and $B_{j\,0} = g_j(0)$ for the rest of the paper. With $x^{[k]}$ we denote the k-th Kronecker Product. Thus, Eq.3 can be equivalently written in the form

$$\dot{x} = f(x) + g(x)u \equiv \sum_{k=1}^{\infty} A_k x^{[k]} + \sum_{j=1}^{m}\sum_{k=1}^{\infty} B_{j\,k} x^{[k]} u_j \tag{5}$$

We will focus on a finite order polynomial approximation of the nonlinear system of order p_f for $f(x)$ and p_g for $g_j(x)$. Without loss of generality we assume that $p_f = p_g + 1 = p$.

$$\dot{x} \simeq \sum_{k=1}^{p} A_k x^{[k]} + \sum_{j=1}^{m}\sum_{k=0}^{p-1} B_{j\,k} x^{[k]} u_j \tag{6}$$

To linearize the system of Eq.5, we compute the dynamic behavior of the terms $x^{[k]}$ as follows:

$$\frac{d(x^{[k]})}{dt} = \sum_{i=1}^{p-k+1} A_{k,i} x^{[i+k-1]} + \sum_{j=1}^{m}\sum_{i=0}^{p-k} B_{j\,k,i} x^{[i+k-1]} u_j \tag{7}$$

$$\dot{x}_{\otimes} = \begin{bmatrix} A_{1,1} & A_{1,2} & \cdots & A_{1,p} \\ 0 & A_{2,1} & \cdots & A_{2,p-1} \\ 0 & 0 & \cdots & A_{3,p-2} \\ \cdots & \cdots & \cdots & \cdots \\ 0 & 0 & \cdots & A_{p,1} \end{bmatrix} x_{\otimes} + \sum_{j=1}^{m} \left\{ \begin{bmatrix} B_{j_{1,1}} & B_{j_{1,2}} & \cdots & B_{j_{1,p-1}} & 0 \\ B_{j_{2,0}} & B_{j_{2,1}} & \cdots & B_{j_{2,p-2}} & 0 \\ 0 & B_{j_{3,0}} & \cdots & B_{j_{3,p-3}} & 0 \\ \cdots & \cdots & \cdots & \cdots & \cdots \\ 0 & 0 & \cdots & B_{j_{p,0}} & 0 \end{bmatrix} x_{\otimes} u_j + \begin{bmatrix} B_{j_{1,0}} \\ 0 \\ 0 \\ \cdots \\ 0 \end{bmatrix} u_j \right\} \quad (8)$$

where $A_{k,i} = \sum_{l=0}^{k-1} I_n^{[l]} \otimes A_i \otimes I_n^{[k-1+l]}$ and $B_{j_{k,i}}$ is defined similarly.

Defining $x_{\otimes} = [x^T {x^{[2]}}^T \cdots {x^{[p]}}^T]^T$, the system of Eq.7 can be written in the following bilinear form

$$\dot{x}_{\otimes} = \mathcal{A} x_{\otimes} + \sum_{j=1}^{m} \left[\mathcal{B}_j x_{\otimes} u_j + \mathcal{B}_{j_0} u_j \right] \quad (9)$$

where $\mathcal{A}$, $\mathcal{B}_j$ and $\mathcal{B}_{j_0}$ are matrices of appropriate form, shown in Eq.8. The presented operation, also known as Carleman linearization [12], presents us with the basis for the identification of the system behavior. We proceed to compute off-line the unknown parameters of the model.

Remark 1: Note that due to the linearization operation, it appears there is a geometric increase of the number of parameters that need be identified. Under assumptions of continuity of the unidentified functions $f(x)$ and $g(x)$, the number of parameters to be identified can be drastically reduced.

2) Off-line identification: Initially Recursive Projection Method [17] is applied to the process simulator to identify the, possibly unstable, target stationary state of the process and the slow eigendirections in the neighborhood of the stationary state. Due to the nature of RPM and the simulator, discrete-time linearizations of the open-loop process model also become available.

In [4] we presented the derivation of closed-loop linear discrete-time models. The RPM identified model is of the form

$$x_{sn+1} = F x_{sn} + D u_n \quad (10)$$

where $x_s \in \mathbb{C}^n$ is a representation of the slow evolving eigendirections of the process of Eq.1, $F \in \mathbb{C}^{n \times n}$ describes their discrete-time linearized dynamics around the stationary-state, $u \in \mathbb{R}^m$ is the vector of the manipulated inputs and $CH \in Cset^{n \times m}$ approximates the linearized effect of the m control actuators on the slow mode dynamics. D is defined as $D = V_F [V^* V]^{-1} V^* H$, where $V \in \mathbb{C}^{N \times n}$ denotes the matrix containing as columns the M slow eigenvectors (identified and approximated through RPM), $V_F \in \mathbb{C}^{n \times n}$ is the matrix with columns the corresponding eigenvectors of F (in the same order, with respect to the eigenvalues, as in V) and $H \in \mathbb{C}^{N \times m}$ is the matrix containing the numerically computed partial derivatives of $\mathcal{L}(x) + f(x)$ of Eq.1 with respect to the action of the m control actuators. The continuous-time behavior of the linearized slow subsystem can be inferred from Eq.10 and is $A_1 = (1/T) V_F ln(V_F^{-1} F V_F) V_F^{-1}$, $D = \int_0^T exp[A_1(T-\tau)] d\tau B_0 \Rightarrow B_0 = (F - I)^{-1} A_1 D$, where $B_0 = [B_{10}\ B_{20}\ \cdots\ B_{m0}]$ and T is the reporting horizon of the microscopic simulations.

Following the identification of the system linearization, we proceed to the off-line identification of $\mathcal{A}$ and $\mathcal{B}_j$ in a sequential manner.

Open-loop behavior identification First, M_{ol} microscopic simulations are employed to generate an ensemble Y^{ol} of snapshots of the process evolution for a variety reporting horizons, time-length of simulation and initial conditions for $u_j \equiv 0,\ \forall j = 1, \ldots, m$. Care must be taken so that the reporting horizon of the simulations is large enough, such that it can be ensured that the fast dynamics of the process have become negligible. The snapshots of each different simulation run are used to compute the slow-system modes x and their representation for the Carleman linear form of Eq.9 $x_{\otimes}$, denoted as $y_{il} \in Y^{ol},\ i = 0, \ldots, n_{f_l},\ l = 1, \ldots M_{ol}$, with T_l the associated reporting horizon, and $n_{f_l} T_l$ the final simulation time. Eq.9 for $u_j \equiv 0,\ \forall j = 1, \ldots, m$ can be solved analytically and the solution is $x_{\otimes}(t) = exp(\mathcal{A}t) x_{\otimes}(0)$.

We obtain an estimate of the unknown parameters of $\mathcal{A}$ through the solution of an optimization problem, formulated as an unconstrained *nonlinear optimization program*, which can be subsequently solved using iterative search methods such as SQP.

$$\begin{aligned} & min_{\mathcal{A}} \left[\sum_{l=1}^{M_{ol}} \sum_{i=1}^{n_{f_l}} (y_{il} - x_{i,l})^2 \right],\ y_{il} \in Y^{ol} \\ & \text{s.t.} \\ & x_{i,l} = exp(\mathcal{A}(iT_l)) y_{0l}, \\ & \forall i = 1, \ldots, n_{f_l},\ \ \forall l = 1, \ldots, M_{ol} \end{aligned} \quad (11)$$

Closed-loop behavior identification Once A of Eq.9 has been identified we can proceed with the identification of the system response to manipulated input excitation. Furthermore, the effect of each manipulated input can be estimated independently.

Microscopic simulations are employed to generate m ensembles Y_j^{cl} of snapshots of the system during the process evolution for a variety of reporting horizons, time-length of simulation and random manipulated variable profiles $u_j(t) = u_{j_i}(H(iT_l - t) - H(t - (i-1)T_l),\ \forall j = 1, \ldots, m$ ($H(\cdot)$ denotes the Heaviside function) and initial condition at the stationary state ($x_{\otimes}(0) = 0$). Care must be taken so that the rate of change of the manipulated inputs is constrained so that they do not excite the fast dynamics of the system. The snapshots of each different simulation run are denoted as $y_{il} \in Y_j^{cl},\ i = 0, \ldots, n_{f_l},\ l = 1, \ldots M_{ol}$, with T_l the associated reporting horizon, and $n_{f_l} T_l$ the final simulation time.

The response of the system of Eq.9 to variations of the manipulated input $u_j(t) = u_{j_i}(H(iT_l - t) - H(t-(i-1)T_l)$, $u_k \equiv 0, \forall k \neq j$ with initial condition at the stationary state can be derived recursively at each time interval $t \in ((i-1)T_l, iT_l]$, since

$$\dot{x}_\otimes = [\mathcal{A} + \mathcal{B}_j u_{j_i}]x_\otimes + \mathcal{B}_{j_0} u_{j_i}.$$

The analytical solution of the above equation is

$$\begin{aligned} x_\otimes(t) =& exp([\mathcal{A} + \mathcal{B}_j u_{j_i}](t-(i-1)T_l))x_\otimes((i-1)T_l) \\ &+ \int_{(i-1)T_l}^{t} exp[\mathcal{A} + \mathcal{B}_j u_{j_i}](t-\tau))d\tau\ \mathcal{B}_{j_0} u_{j_i}, \end{aligned}$$

and for $t = iT_l$ we define $x_{il} \equiv x_\otimes(iT_l)$ with

$$\begin{aligned} x_\otimes(iT_l) =& exp([\mathcal{A} + \mathcal{B}_j u_{j_i}]T_l)x_{i-1l} + [\mathcal{A} + \mathcal{B}_j u_{j_i}]^{-1} \\ &\times (exp([\mathcal{A} + \mathcal{B}_j u_{j_i}]T_l) - I)\mathcal{B}_{j_0} u_{j_i}. \end{aligned}$$

Note that $x_{0l} = 0$.

We obtain an estimate of the unknown parameters of matrices $\mathcal{B}_j$ through the solution of j unconstrained NLPs.

$$min_{\mathcal{B}_j} \left[\sum_{l=1}^{M_{cl\,j}} \sum_{i=1}^{n_{f_l}} (y_{il} - x_{i,l})^2 \right],\ y_{il} \in Y_j^{cl}$$

s.t.

$$\begin{aligned} x_{il} =& exp([\mathcal{A} + \mathcal{B}_j u_{j_i}]T_l)x_{i-1l} \\ &+ [\mathcal{A} + \mathcal{B}_j u_{j_i}]^{-1}(exp([\mathcal{A} + \mathcal{B}_j u_{j_i}]T_l) - I)\mathcal{B}_{j_0} u_{j_i}. \end{aligned}$$

$$x_0 = 0$$

$$\forall i = 1, \ldots, n_{f_j},\ \ \forall j = 1, \ldots, M_{ol} \tag{12}$$

Remark 2: A way to approximately estimate the shortest reporting horizon that will be used for the creation of the ensembles is to employ Arnoldi method [6] and estimate the largest eigenvalue of the non identified fast subsystem. Subsequently the shortest reporting horizon must be such that it falls in the separation gap between the fast and slow dynamics.

B. Output feedback controller design

In the present paper we focus on systems where $\mathcal{B}(x) \equiv \mathcal{B}$ in Eq.1 (in [1] a detailed controller design methodology is presented for the general developed process model). In this case, $\mathcal{B}_j \equiv 0$ in Eq.9, which implies we can design output feedback controllers, by designing Linear Quadratic Regulators (LQRs) for Eq.9, and subsequently linking them with dynamic observers. Note that, even though we employ linear controller design methodologies, the resulting controllers of Eq.1 are nonlinear, since the controllers employ polynomial terms up to order p.

We initially design state-feedback continuous-time LQRs by solving an optimal control problem with cost function:

$$J = \int_0^\infty {x_\otimes}^* Q x_\otimes + u^*(t) R u(t)\ dt \tag{13}$$

where Q, R are positive semidefinite matrices and $u = [u_1\ u_2\ \ldots\ u_m]^T$. We use the algebraic Riccati equation to solve the infinite time optimization problem and compute the optimal feedback controller gain P_c [**?**]:

$$\begin{aligned} Q &= \mathcal{A}^* P - P\mathcal{A} + P\mathcal{B}_0 R^{-1} \mathcal{B}_0^* P \\ P_c &= -R^{-1}\mathcal{B}_0^* P \end{aligned} \tag{14}$$

where $\mathcal{B}_0 = [\mathcal{B}_{10}\ \mathcal{B}_{20}\ \cdots\ \mathcal{B}_{m0}]$ and the control action is given from $u(t) = P_c x(t)$.

We derive a state observer for the process

$$\begin{aligned} \dot{\tilde{x}}_\otimes &= \mathcal{A}\tilde{x}_\otimes + \mathcal{B}_0 u + L(y_s - y_m) \\ y_s &= [\mathcal{S}\ \ \mathbf{0}_{q\times(\sum_{i=2}^{p} n^i)}]\tilde{x}_\otimes \end{aligned} \tag{15}$$

where $\tilde{x}_\otimes$ is the observer state, y_m is the measurement, $\mathcal{S}$ can be constructed from the sensor shape function and the representation of the eigenmode, and $\mathbf{0}_{N\times M}$ represent a matrix of size $N \times M$ with zero elements. L is the observer gain (computed such that the observer is stable)

We combine the state feedback LQR with the derived state observer to obtain the following output feedback controller:

$$\begin{aligned} \dot{\tilde{x}}_\otimes &= \mathcal{A}\tilde{x}_\otimes + \mathcal{B}_0 u + L(y_s - y_m) \\ y_s &= [\mathcal{S}\ \ \mathbf{0}_{q\times(\sum_{i=2}^{p} n^i)}]\tilde{x}_\otimes \\ u &= P_c \tilde{x}_\otimes \end{aligned} \tag{16}$$

IV. Application to the FitzHugh-Nagumo equation

The proposed controller design approach is validated using a timestepper of the FitzHugh-Nagumo (FHN) equation, a widely used model of wavy behavior in excitable media in biology [10] and chemistry [21], with the following closed-form description:

$$\begin{aligned} \frac{\partial v}{\partial t} &= \frac{\partial^2 v}{\partial z^2} + v - w - v^3 + b(z)u(t) \\ \frac{\partial w}{\partial t} &= \delta \frac{\partial^2 w}{\partial z^2} + \epsilon(v - p_1 w - p_0) \\ y_m(t) &= s(z)v(t) \end{aligned} \tag{17}$$

subject to the boundary conditions:

$$\frac{\partial v}{\partial z}|_0 = \frac{\partial v}{\partial z}|_L = 0, \quad \frac{\partial w}{\partial z}|_0 = \frac{\partial w}{\partial z}|_L = 0 \tag{18}$$

and the initial conditions:

$$v(0,z) = v_0(z), \quad w(0,z) = x_0(z) \tag{19}$$

where $v(t,z),\ w(t,z) \in \mathbb{R}$ are the system variables, $u(t) \in \mathbb{R}^3$ is the vector of manipulated variables, $y_m(t) \in \mathbb{R}^3$ is the vector of measurements, t is the time, z is the spatial coordinate, $b(z)$ is a row vector describing the distribution function of the control actuators, ϵ, δ, p_1, p_0 are process parameters and L is the length of the spatial domain. We assume that three control actuators are available:

$$b(z) = [g(z, 0.25L)\ \ g(z, 0.50L)\ \ g(z, 0.75L)]$$

where $g(z,\zeta) = exp(-0.3(z-\zeta)^2)$; note that this choice of actuator influence functions extends over the entire spatial

domain of the process. We also assume that three point measurements of $v(t,z)$ are available, of the form:

$$s(z) = [\delta(z, 0.25L) \;\; \delta(z, 0.50L) \;\; \delta(z, 0.75L)]^T$$

where $\delta(\cdot)$ denotes the delta function. In the following simulations, the initial conditions were chosen as $v_0 = 0.5cos(\pi z/L)$ and $w_0 = 0.5cos(\pi z/L)$.

TABLE I

PROCESS PARAMETERS

L	20	δ	4.0	p_1	2.0
T	0.5	ϵ	0.017	p_0	-0.03

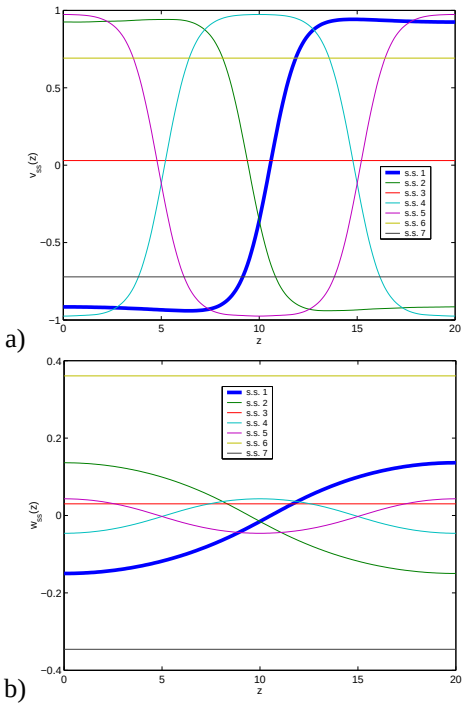

Fig. 1. Open-loop steady states of the FHN equation. (a) v, (b) w.

The FHN exhibits multiple steady-state solutions (spatially uniform as well as spatially nonuniform) and spatially nonuniform periodic solutions, depending on the values of the process parameters. For the specific parameter values shown in Table I, the system has at least four spatially nonuniform and three spatially uniform steady-states, presented in Figures 1a and 1b, for v and w respectively.

Using Galerkin's method with the (analytically derived) eigenfunctions of the spatial operator, we discretize the system in the spatial domain. Linearizing the discretized FHN in the neighborhood of the steady-states and computing the eigenvalues we conclude that the system is locally unstable in the neighborhood of steady states one, two and three, and locally stable in the neighborhood of steady states four, five, six and seven. Furthermore, simulating Eq.17 with $u(t) \equiv 0$ and initial conditions far from the stable steady-states, we observe FHN converges to a locally stable, spatially nonuniform periodic orbit shown in Figures 2a and 2b for $v(t)$ and $w(t)$ respectively. We now focus our attention to

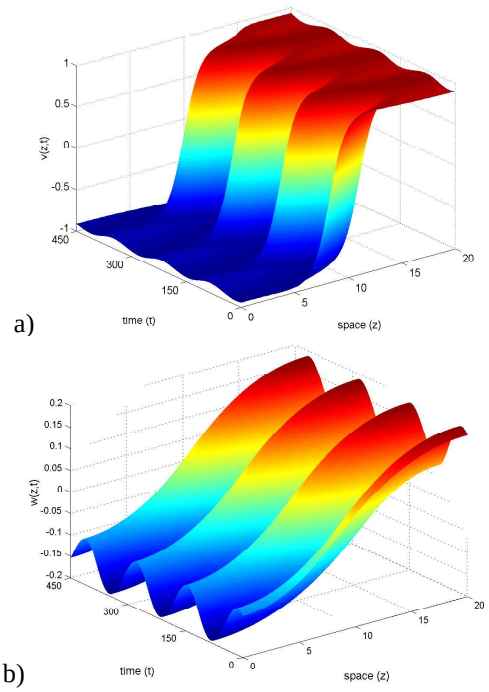

Fig. 2. Open-loop stable periodic orbit of FHN equation. (a) v, (b) w.

steady-state one depicted as thick lines in Figures 1a and 1b for v and w respectively (denoted as $x_{ss,1}$ for the rest of the section). We observe in Table II that there is a finite number of eigenvalues close to the imaginary axis, while an infinite number of them grow towards negative infinity. Moreover we observe that a large spectral gap exists between two consecutive eigenvalues. This time-scale separation suggests that a few dominant modes may be able to capture the long term dynamics of the open-loop process.

We now switch to the alternative, kinetic theory based LB-BGK scheme, which has been constructed so that its zeroth moment fields approximately satisfy the FHN equation [21], [4]. A coarse time-stepper with a time-reporting horizon of $T = 0.5$ was constructed for this scheme. It combined lifting, from zeroth moment fields to full LB state fields (employing a local equilibrium assumption), LB-BGK "mesoscopic" evolution, and restriction back to zeroth moments corresponding to v and w. The combination of coarse LB-BGK timestepper with RPM located the target coarse stationary state and inferred the coarse stability properties of the process through estimates of the leading coarse eigenvalues/vectors. Through algebraic manipulations, an approximate linear continuous time coarse slow subsystem in its neighborhood was also computed.

Specifically, using as an initial guess the stable coarse stationary profile at $\epsilon = 0.1$ and $\epsilon = 0.11$, we converged to the unstable nonuniform coarse stationary profile at the target value of $\epsilon = 0.017$, which lies beyond the Hopf bifurcation at $\epsilon = 0.019$. We also approximated the coarse slow eigenvalues, their respective eigenvectors and estimated matrix F of Eq.10 for the coarse slow subsystem. Depending on the detailed RPM implementation

parameters, and -in particular- on the convergence tolerance, the dimension of the recursively identified coarse slow subspace required to achieve convergence ranged from 2 to 4. The reader may refer to [17], [11], [4], [1] for a detailed analysis on the effect of RPM parameters on the identification of the slow subsystem. In Table II, we present the open-loop eigenvalues of the coarse system and compare with the ones computed based on the FHN discretization. We observe that the eigenvalues computed from RPM are in good agreement with the FHN ones, being within the error tolerance value used by RPM. The real part of the corresponding (discretized in space) eigenfunctions are presented in Figure 3a for $v(z)$ and Figure 3a for $w(z)$. We observe that they are spatially nonuniform and smooth functions of time and that they satisfy the boundary conditions of the FHN equation.

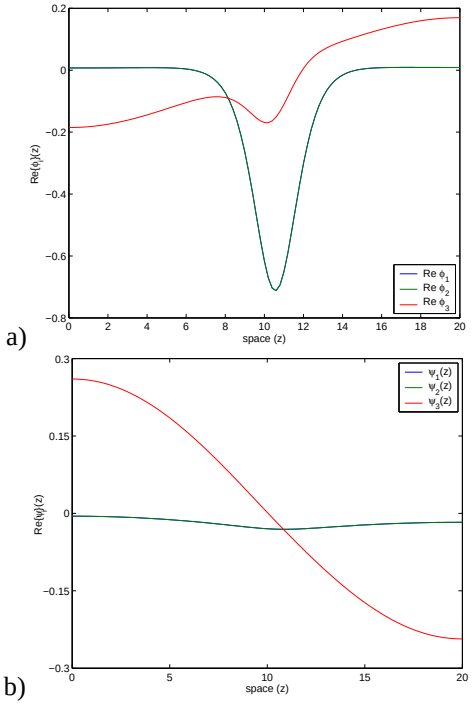

Fig. 3. Spatial profile of the real part of the RPM identified eigenfunctions in the neighborhood of $x_{ss,1}$. (a) v, (b) w.

Following the coarse open-loop analysis, we computed the coarse process response to actuators' perturbations, and subsequently obtained a linearized expression of their effect on the slow discrete-time subsystem (matrix F of Eq.10).

TABLE II

EIGENVALUES OF LINEARIZED FHN IN THE NEIGHBORHOOD OF $x_{ss,1}$

Open-loop		Closed-loop [LQR]
PDE linearization	LB-RPM	[3:LB-RPM]
$0.00048 + 0.04665i$	-0.00079+.02492I	-0.01592
$0.00048 - 0.04665i$	-0.00079-.02492I	-0.07171
-0.14428	-0.07289	-0.1237
-0.21245	–	-0.2002
-0.42501	–	-0.4743

Since two of the identified eigenvalues lie close to the imaginary axis our control objective becomes to place the closed-loop eigenvalues corresponding to the critically stable slow eigenmodes away from the imaginary axis. To retain the time-scale separation between the slow and the fast subsystems, the resulting closed-loop eigenvalues are placed close to the third identified slow eigenvalue. Such an objective will also induce relatively small control actions prescribed by the controller to avoid exciting the fast dynamics of the process.

We designed an LQR continuous-time controller for the RPM identified linear model solving the Riccati equation with cost function weights in Eq.13 $Q = 0.5I_{3\times3}$, and $R = 10I_{3\times3}$. The dominant eigenvalues of the closed-loop system under the computed LQR were placed at $\mu_1 = -.274$, $\mu_2 = -0.106$ and $\mu_3 = -.0897$.

In Table II we present the eigenvalues of the closed-loop FHN in the neighborhood of $x_{ss,1}$ and compare them with the eigenvalues of the open-loop system. We observe that the eigenvalues of the closed-loop system are negative implying that the closed loop FHN is stabilized, and the time-scale separation between the slow eigenmodes and the fast ones (gap between the fourth and fifth eigenmodes) persists: spillover did not change the dimension of the closed-loop slow subsystem. We also observe that the controller fails to assign all the eigenvalues at the desired locations, in part due to spillover, and in part due to the inaccuracy of coarse slow eigenvalue/eigenvector estimates (which, however, can be further refined).

In Figure 4a we present the temporal profiles of the control action. We observe that the control action tends to zero as time progresses, and it achieves stabilizing the FHN process at $x_{ss,1}$ without chattering. The effect of the LQR controller on the dynamics is shown in Figure 4b where the time-profile of the L_2 norm of the FHN converges to the stationary value rapidly and smoothly. In Figure 4c we present the effect of the control action on the deviations of the measurements y_m from their respective values at the target stationary state. We observe that they converge to zero rapidly and without chattering. Figures 5a and 5b present the spatiotemporal profiles of the zeroth moments of the LB-BGK that correspond to $v(z,t)$ and $w(z,t)$ respectively. Due to space limitations, the presentation of the nonlinear controller design was omitted. A detailed description of the nonlinear controller design for the FHN is presented in [1].

V. CONCLUSIONS

A continuous-time feedback controller design methodology was developed for distributed processes, whose dynamic behavior can be described by microscopic evolution rules. Employing the micro-Galerkin method to bridge the gap between the microscopic-level evolution rules and the "coarse" process behavior, "coarse" process steady states were estimated and nonlinear process models were identified off-line through the solution of a series of nonlinear programs. Subsequently, optimal feedback controllers were designed, on the basis of the nonlinear process model, that enforce stability in the closed-loop system. The

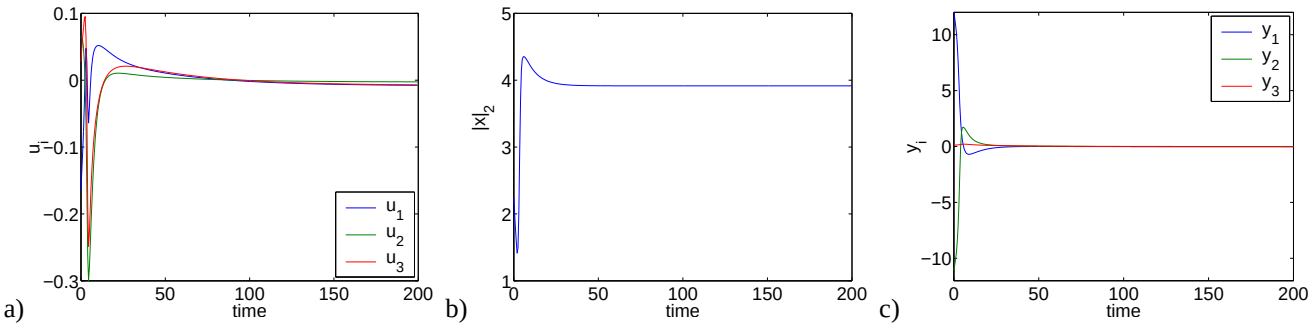

Fig. 4. Time profiles: (a) control action of 3rd order LB-RPM LQR (b) L_2 norm of closed-loop FHN under 3rd order LB-RPM LQR, (c) measurements of closed-loop FHN under 3rd order LB-RPM LQR

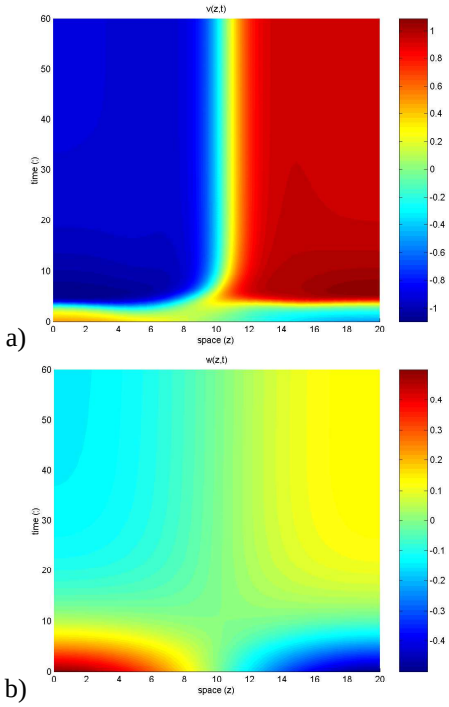

Fig. 5. Closed-loop FHN evolution under 3rd order LB-RPM LQR ($v_0 = 0.5cos(\pi z/L)$, $w_0 = 0.5cos(\pi z/L)$). (a) v and (b) w.

method was used to control a system of coupled nonlinear one-dimensional PDEs (the FitzHugh-Nagumo equations), widely used to describe the formation of patterns in reacting and biological systems. Employing kinetic theory based microscopic realizations of the process, linear quadratic regulators were designed that stabilized the FHN at an unstable, nonuniform in space, steady state, in the presence of open-loop oscillatory behavior.

REFERENCES

[1] A. Armaou. Output feedback control of distributed processes via microscopic simulations, submitted. *Comp. & Chem. Engng.*, 2004.

[2] A. Armaou and P. D. Christofides. Wave suppression by nonlinear finite-dimensional control. *Chem. Eng. Sci.*, 55:2627–2640, 2000.

[3] A. Armaou and P. D. Christofides. Finite-dimensional control of nonlinear parabolic PDEs with time-dependent spatial domains using empirical eigenfunctions. *Int. J. Appl. Math. & Comp. Sci.*, 11:287–317, 2001.

[4] A. Armaou, C. I. Siettos, and I. G. Kevrekidis. Time-steppers and coarse control of distributed microscopic processes. *Int. J. Rob. & Nonl. Control*, 14:89–111, 2004.

[5] J. Q. Broughton, F. F. Abraham, N. Bernstein, and E. Kaxiras. Concurrent coupling of length scales: Methodology and application. *Phys. Rev. B*, 60:2391–2403, 1999.

[6] K. N. Christodoulou and L. E. Scriven. Finding leading modes of a viscous free surface flow: An assymetric generalized eigenproblem. *J. Sci. Comp.*, 3:355–405, 1988.

[7] P. D. Christofides. *Nonlinear and Robust Control of Partial Differential Equation Systems: Methods and Applications to Transport-Reaction Processes*. Birkhäuser, New York, 2001.

[8] M. A. Gallivan and Murray R. M. Reduction and identification methods for markovian control systems, with application to thin film deposition. *Int. J. Rob. & Nonlin. Con.*, 14:113–132, 2004.

[9] A. E. Ismail, G. C. Rutledge, and G. Stephanopoulos. Multiresolution analysis in statistical mechanics. I. using wavelets to calculate thermodynamic properties. *J. Chem. Phys.*, 118:4414–4423, 2003.

[10] J. Keener and J. Sneyd. *Mathematical physiology*. Springer-Verlag, New York, 1998.

[11] I. G. Kevrekidis, C. W. Gear, J. M. Hyman, P. G. Kevrekidis, O. Runborg, and K. Theodoropoulos. Equation-free multiscale computation: enabling microscopic simulators to perform system-level tasks, submitted. *Comm. Math. Sciences*, 1:715–762, 2003.

[12] K. L. Kowalski and W.-H. Steeb. *Nonlinear Dynamical Systems and Carleman Linearization*. World Scientific Publishing Company, Singapore, 1991.

[13] Y. Lou and P. D. Christofides. Estimation and control of surface roughness in thin film growth using kinetic Monte-Carlo models. *Chem. Eng. Sci.*, 58:3115–3129, 2003.

[14] Y. Lou and P. D. Christofides. Feedback control of growth rate and surface roughness in thin film growth. *AIChE J.*, 49:2099–2113, 2003.

[15] H. M. Park and D.H. Cho. The use of the Karhunen-Loeve decomposition for the modeling of distributed parameter systems. *Chem. Eng. Sci.*, 51:81–98, 1996.

[16] S. Raimondeau and D. G. Vlachos. Low-dimensional approximations of multiscale epitaxial growth models for microstructure control of materials. *J. Comp. Phys.*, 160:564–576, 2000.

[17] G. M. Shroff and H. B. Keller. Stabilization of unstable procedurers: The Recursive Projection Method. *SIAM J. Numer. Anal.*, 30:1099–1120, 1993.

[18] S. Shvartsman and I. G. Kevrekidis. Nonlinear model reduction for control of distributed parameter systems. *AIChE J.*, 44:1579–1595, 1998.

[19] C. I. Siettos, A. Armaou, A. G. Makeev, and I. G. Kevrekidis. Microscopic/stochastic timesteppers and 'coarse' control: a kinetic Monte Carlo example. *AIChE J.*, 49:1922–1926, 2003.

[20] C. I. Siettos, C. C. Pantelides, and I. G. Kevrekidis. Enabling dynamic process simulators to perform alternative tasks: A time-stepper based toolkit for computer-aided analysis. *Ind. Eng. Chem. Research*, 42:6795–6801, 2003.

[21] K. Theodoropoulos, Y.-H. Qian, and I.G. Kevrekidis. "Coarse" stability and bifurcation analysis using timesteppers: a reaction diffusion example. *Proc. Natl. Acad. Sci.*, 97:9840–9843, 2000.